

# Collider signatures for unparticle

Kingman Cheung<sup>1,2</sup>, Wai-Yee Keung<sup>3</sup>, and Tzu-Chiang Yuan<sup>1,2</sup>

<sup>1</sup> Department of Physics, National Tsing Hua University, Hsinchu, Taiwan

<sup>2</sup> Physics Division, National Center for Theoretical Sciences, Hsinchu, Taiwan

<sup>3</sup> Department of Physics, University of Illinois at Chicago, Chicago IL 60607-7059, U.S.A.

**Abstract.** We summarize the works presented in Refs. [1,2] on collider phenomenology of the unparticle physics associated with an exact scale invariant sector possessing a non-trivial infrared fixed point at a high energy scale. We give highlights on the motivations of unparticle and derivation of the phase space and the unparticle propagator. We study two categories of phenomenology: (i) real emission of unparticle that gives rise to peculiar missing energy signatures, and (ii) virtual exchange of unparticle that interferes with the standard model amplitudes.

**PACS.** 14.80.-j Other particles (including hypothetical) – 12.90.+b Miscellaneous theoretical ideas and models

## 1 Introduction

Scale invariance is a powerful concept that is widely used in various disciplines of physics. However, it is manifestly broken by the masses of elementary particles in the part of the world known to us. Nevertheless, it is conceivable that at a much higher scale there may exist a nontrivial scale invariant sector with an infrared fixed point that we have not yet probed experimentally.

Recently, Georgi [3] motivated by the Banks-Zaks ( $\mathcal{BZ}$ ) theory [4] suggested that a scale invariant sector behaves rather peculiarly from the perspective of particle physics. An operator  $\mathcal{O}_U$  with a general non-integral scaling dimension  $d_U$  in a scale invariant sector has a mass spectrum looked like a  $d_U$  number of invisible massless particles, coined as unparticle  $\mathcal{U}$  by Georgi. Unparticle does not have a fixed invariant mass but instead a continuous mass spectrum. The most interesting feature is that real production of unparticle, described by an effective field theory, can give rise to peculiar missing energy distributions because of the possible non-integral values of  $d_U$ .

Shortly after Georgi's work [3], the propagator for the unparticle was worked out independently in [5] and [1]. An unusual phase in the unparticle propagator was discovered by both groups and the interesting interference patterns between the amplitude of  $s$ -channel unparticle exchange and those from the SM were studied. In this proceedings, we summarize the collider phenomenology presented in Refs. [1,2], while there have been a large amount of recent literature on this subject but we have to skip because of space.

## 2 Formalism

Effective field theory approach was adopted in studying the phenomenology of unparticle [3]. The  $\mathcal{BZ}$  sector interacts with the SM fields through the exchange of a connector sector at a high mass scale  $M_U$ . Below  $M_U$  non-renormalizable operators suppressed by inverse powers of  $M_U$  are induced. Generically, operators are of the form

$$\frac{1}{M_U^{d_{SM}+d_{\mathcal{BZ}}-4}} \mathcal{O}_{SM} \mathcal{O}_{\mathcal{BZ}} , \quad (1)$$

where  $\mathcal{O}_{SM}$  and  $\mathcal{O}_{\mathcal{BZ}}$  represent local operators constructed out of SM and  $\mathcal{BZ}$  fields with scaling dimensions  $d_{SM}$  and  $d_{\mathcal{BZ}}$ , respectively. Renormalization effects in the scale invariant  $\mathcal{BZ}$  sector induce dimensional transmutation [6] at an energy scale  $\Lambda_U$ . Below  $\Lambda_U$  matching conditions must be imposed onto the operator (1) to match a new set of operators having the form

$$C_{\mathcal{O}_U} \frac{\Lambda_U^{d_{\mathcal{BZ}}-d_U}}{M_U^{d_{SM}+d_{\mathcal{BZ}}-4}} \mathcal{O}_{SM} \mathcal{O}_U , \quad (2)$$

where  $d_U$  is the scaling dimension of the unparticle operator  $\mathcal{O}_U$  and  $C_{\mathcal{O}_U}$  is a coefficient function fixed by the matching. We assume that exact scale invariance survives all the way down to the electroweak scale.

It was demonstrated in [3] that scale invariance can be used to fix the two-point functions of the unparticle operators. The spectral density  $\rho_U(P^2)$  is then given by

$$\begin{aligned} \rho_U(P^2) &= \int d^4x e^{iP \cdot x} \langle 0 | \mathcal{O}_U(x) \mathcal{O}_U^\dagger(0) | 0 \rangle \\ &= A_{d_U} \theta(P^0) \theta(P^2) (P^2)^\alpha \end{aligned} \quad (3)$$

where  $\alpha$  is fixed by scale invariance to be  $(d_U - 2)$ , and  $A_{d_U}$  is normalized to interpolate the  $d_U$ -body phase space of massless particle [3], given by

$$A_{d_U} = \frac{16\pi^2\sqrt{\pi}}{(2\pi)^{2d_U}} \frac{\Gamma(d_U + \frac{1}{2})}{\Gamma(d_U - 1)\Gamma(2d_U)}. \quad (4)$$

The most important feature of unparticle is that  $d_U$  can take on non-integral values, and so we can imagine something similar to fractional particles.

## 2.1 Unparticle propagators

The derivation of the virtual unparticle propagator is also based on scale invariance. Without loss of generality we consider a scalar propagator. The extensions to spin-1 and spin-2 propagators simply include the appropriate spin structures. The Feynman propagator  $\Delta_F(P^2)$  of the unparticle is determined by the spectral formula

$$\Delta_F(P^2) = \frac{1}{2\pi} \int_0^\infty \frac{R(M^2)dM^2}{P^2 - M^2} - i\frac{1}{2}R(P^2)\theta(P^2) \quad (5)$$

where  $R(M^2) = A_{d_U}(M^2)^{d_U-2}$ . The appropriate form for  $\Delta_F(P^2)$  is  $\Delta_F(P^2) = Z_{d_U}(-P^2)^{d_U-2}$ , where  $Z_{d_U}$  is the factor to be determined. The complex function  $(-P^2)^{d_U-2}$  is analytic for negative  $P^2$ , but needs a branch cut for positive  $P^2$ :

$$(-P^2)^{d_U-2} = \begin{cases} |P^2|^{d_U-2} & \text{if } P^2 \leq 0, \\ |P^2|^{d_U-2} e^{-id_U\pi} & \text{if } P^2 > 0. \end{cases} \quad (6)$$

The factor  $Z_{d_U}$  is determined by comparing with the imaginary part of  $\Delta_F(P^2)$  for a time-like momentum ( $P^2 > 0$ ) and given by

$$Z_{d_U} = \frac{A_{d_U}}{2\sin(d_U\pi)}. \quad (7)$$

## 2.2 Effective interactions

A few common effective interactions that satisfy the standard model gauge symmetry for the scalar, vector, and tensor unparticle operators with SM fields are given, respectively, by

$$\lambda_0 \frac{1}{\Lambda_U^{d_U-1}} \bar{f} f O_U, \quad \lambda_0 \frac{1}{\Lambda_U^{d_U}} G_{\alpha\beta} G^{\alpha\beta} O_U, \quad (8)$$

$$\lambda_1 \frac{1}{\Lambda_U^{d_U-1}} \bar{f} \gamma_\mu f O_U^\mu, \quad \lambda_1 \frac{1}{\Lambda_U^{d_U-1}} \bar{f} \gamma_\mu \gamma_5 f O_U^\mu, \quad (9)$$

$$-\frac{1}{4} \lambda_2 \frac{1}{\Lambda_U^{d_U}} \bar{\psi} i \left( \gamma_\mu \overleftrightarrow{D}_\nu + \gamma_\nu \overleftrightarrow{D}_\mu \right) \psi O_U^{\mu\nu},$$

$$\lambda_2 \frac{1}{\Lambda_U^{d_U}} G_{\mu\alpha} G_\nu^\alpha O_U^{\mu\nu}, \quad (10)$$

where the covariant derivative  $D_\mu = \partial_\mu + ig \frac{\tau_a}{2} W_\mu^a + ig' \frac{Y}{2} B_\mu$ ,  $G^{\alpha\beta}$  denotes the gauge field strength (gluon,

photon and weak gauge bosons), and  $\lambda_i$  are dimensionless effective couplings  $C_{O_U^i} \Lambda_U^{d_{BZ}} / M_U^{d_{SM}+d_{BZ}-4}$ .

Virtual exchange of unparticle corresponding to the vector operator  $O_U^\mu$  between two fermionic currents can result in 4-fermion interactions [1, 2, 5]

$$\mathcal{M}_1^{4f} = \lambda_1^2 Z_{d_U} \frac{1}{\Lambda_U^2} \left( -\frac{P_U^2}{\Lambda_U^2} \right)^{d_U-2} \bar{f}_2 \gamma_\mu f_1 \bar{f}_4 \gamma^\mu f_3 \quad (11)$$

The phase factor  $\exp(-i\pi d_U)$  for time-like momentum  $P_U^2 > 0$  can give rise to nontrivial interference patterns with SM amplitudes. Another important feature is that the high energy behavior of the amplitude scales as  $(s/\Lambda_U^2)^{d_U-1}$ . For  $d_U = 1$  the tree amplitude behaves like that of a massless photon exchange, while for  $d_U = 2$  the amplitude reduces to the conventional 4-fermion contact interaction [7]. If  $d_U$  is between 1 and 2, say 3/2, the amplitude has the unusual behavior of  $\sqrt{s}/\Lambda_U$  at high energy. If  $d_U = 3$  the amplitude's high energy behavior becomes  $(s/\Lambda_U^2)^2$ , which resembles that of Kaluza-Klein tower of gravitons. One can also consider a spin-2 unparticle exchange between a pair of fermionic currents, but it is suppressed by  $(s/\Lambda_U)^2$  relative to that induced by spin-1 unparticle operator.

## 3 Collider Phenomenology

### 3.1 Real emissions

*Mono-photon events in  $e^-e^+$  collisions:* The energy spectrum of the mono-photon from the process  $e^-e^+ \rightarrow \gamma U$  can be used to probe the unparticle sector. Its cross section is given by

$$d\sigma = \frac{1}{2s} |\overline{\mathcal{M}}|^2 \frac{A_{d_U}}{16\pi^3 \Lambda_U^2} \left( \frac{P_U^2}{\Lambda_U^2} \right)^{d_U-2} E_\gamma dE_\gamma d\Omega \quad (12)$$

with the matrix element squared

$$|\overline{\mathcal{M}}|^2 = 2e^2 Q_e^2 \lambda_1^2 \frac{u^2 + t^2 + 2sP_U^2}{ut}. \quad (13)$$

The  $P_U^2$  is related to the energy of the photon  $E_\gamma$  by the recoil mass relation,  $P_U^2 = s - 2\sqrt{s} E_\gamma$ . The mono-photon energy spectrum is plotted in Fig. 1 for various choices of  $d_U$ . The sensitivity of the scaling dimension to the energy distribution can be easily discerned.

$Z \rightarrow f\bar{f}U$ : The decay width for the process can be easily obtained as

$$\frac{1}{\Gamma_{Z \rightarrow f\bar{f}}} \frac{d\Gamma(Z \rightarrow f\bar{f}U)}{dx_1 dx_2 d\xi} = \frac{\lambda_1^2}{8\pi^3} g(1-x_1, 1-x_2, \xi) \times \frac{M_Z^2}{\Lambda_U^2} A_{d_U} \left( \frac{P_U^2}{\Lambda_U^2} \right)^{d_U-2} \quad (14)$$

where  $\xi = P_U^2/M_Z^2$  and  $x_{1,2}$  are the energy fractions of the fermions  $x_{1,2} = 2E_{f,\bar{f}}/M_Z$ , and the function  $g(z, w, \xi)$  is given in Ref. [1]. In Fig. 2, we plot the normalized decay rate of this process versus the energy fraction  $x_3 = 2 - x_1 - x_2$ . One can see that the shape depends sensitively on the scaling dimension of the unparticle operator.

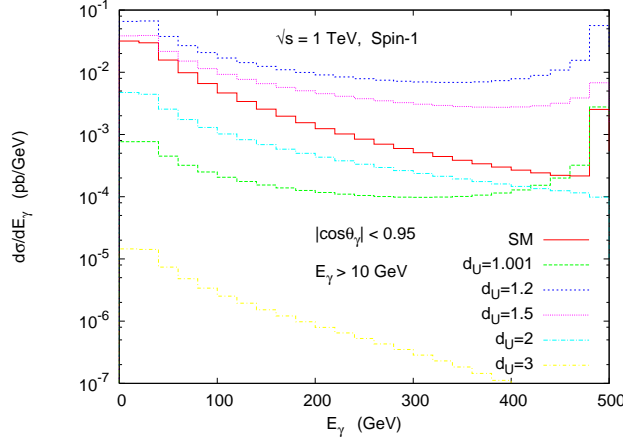


**Fig. 1.** Comparison of photon energy spectrum of  $e^-e^+ \rightarrow \gamma\mathcal{U}$  (spin-1 unparticle) with the SM background  $e^-e^+ \rightarrow \gamma Z^* \rightarrow \gamma\nu\bar{\nu}$  for different values of  $d_{\mathcal{U}} = 1.001, 1.2, 1.5, 2$  and  $3$  at  $\sqrt{s} = 1$  TeV.

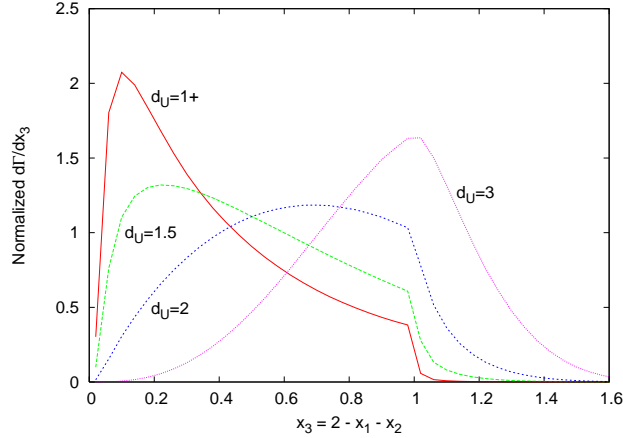


**Fig. 2.** Normalized decay rate of  $Z \rightarrow q\bar{q}\mathcal{U}$  for spin-1 unparticle versus  $x_3 = 2 - x_1 - x_2$  for different values of  $d_{\mathcal{U}} = 1^+, 1.5, 2$ , and  $3$ , where “ $1^+$ ” stands for  $1 + \epsilon$  for a small positive  $\epsilon$ .

### 3.2 Virtual Exchanges

*Drell-Yan* production including the effect of the spin-1 unparticle was first studied in Ref. [1]. The differential cross section is given by

$$\frac{d^2\sigma}{dM_{\ell\ell} dy} = K \frac{M_{\ell\ell}^3}{72\pi s} \sum_q f_q(x_1) f_{\bar{q}}(x_2) \times \left( |M_{LL}|^2 + |M_{LR}|^2 + |M_{RL}|^2 + |M_{RR}|^2 \right), \quad (15)$$

where  $\hat{s} = M_{\ell\ell}^2$  and  $\sqrt{s}$  is the center-of-mass energy of the colliding hadrons.  $M_{\ell\ell}$  and  $y$  are the invariant mass and the rapidity of the lepton pair, respectively, and  $x_{1,2} = M_{\ell\ell} e^{\pm y} / \sqrt{s}$ . The  $K$  factor equals  $1 + \frac{\alpha_s}{2\pi} \frac{4}{3} \left( 1 + \frac{4\pi^2}{3} \right)$ . The reduced amplitude  $M_{\alpha\beta}(\alpha, \beta = L, R)$  is given by

$$M_{\alpha\beta} = \lambda_1^2 Z_{d_{\mathcal{U}}} \frac{1}{\Lambda_{\mathcal{U}}^2} \left( -\frac{\hat{s}}{\Lambda_{\mathcal{U}}^2} \right)^{d_{\mathcal{U}}-2} + \frac{e^2 Q_l Q_q}{\hat{s}}$$

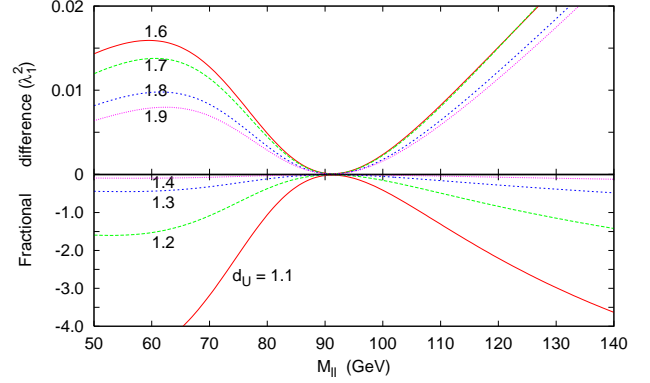


**Fig. 3.** Fractional difference from the SM prediction of the Drell-Yan invariant mass spectrum for various  $d_{\mathcal{U}}$  at the Tevatron in units of  $\lambda_1^2$ . We have chosen  $\Lambda_{\mathcal{U}} = 1$  TeV. The curve for  $d_{\mathcal{U}} = 1.5$  is too close to zero for visibility in the current scale.

$$+ \frac{e^2 g_{\alpha}^l g_{\beta}^q}{\sin^2 \theta_w \cos^2 \theta_w} \frac{1}{\hat{s} - M_Z^2 + i M_Z \Gamma_Z}. \quad (16)$$

This unparticle propagator with the phase factor  $\exp(-i\pi d_{\mathcal{U}})$  interferes with both the real photon propagator and the real and imaginary parts of the unstable  $Z$  boson propagator. This gives rise to interesting interference patterns [5, 1]. Effects from spin-2 unparticle exchanges are suppressed w.r.t. spin-1 exchanges [2]. In Fig. 3, we depict the fractional difference from the SM prediction in units of  $\lambda_1^2$  (with small  $\lambda_1$  while keeping  $\Lambda_{\mathcal{U}} = 1$  TeV) of the Drell-Yan distribution as a function of the invariant mass of the lepton pair for various  $d_{\mathcal{U}}$ .

$e^+e^- \rightarrow f\bar{f}$  production at  $e^-e^+$  colliders can be studied using the amplitude in Eq. (16) with appropriate color-factor modifications for spin-1 unparticle exchange. The differential cross section including the spin-1 unparticle exchange is given by

$$\frac{d\sigma(e^-e^+ \rightarrow f\bar{f})}{d\cos\theta} = \frac{N_c s}{128\pi} \left[ (1 + \cos\theta)^2 (|M_{LL}|^2 + |M_{RR}|^2) + (1 - \cos\theta)^2 (|M_{LR}|^2 + |M_{RL}|^2) \right] \quad (17)$$

The unparticle 4-fermion contact interactions in Eq. (11) can be different for different chiralities of the fermions. It is clear from Eq. (17) that different modifications to  $M_{\alpha\beta}$  can significantly change the angular distribution, because  $M_{LL}$  and  $M_{RR}$  are multiplied by  $(1 + \cos\theta)^2$  while  $M_{LR}$  and  $M_{RL}$  are multiplied by  $(1 - \cos\theta)^2$ . The forward-backward asymmetry can therefore discriminate various chirality couplings.

*Diphoton production* at  $e^-e^+$  and hadronic colliders is very useful to detect unknown resonances that decay into a pair of photons and to search for anomalous diphoton couplings. The spin-2 unparticle can couple to a pair of fermions via the first operator of Eq. (10) and to a pair of photons via the second operator in Eq. (10). The amplitudes are given in Ref. [2]. We show the angular distribution in Fig. 4. In the SM, the angular distribution is very forward with majority

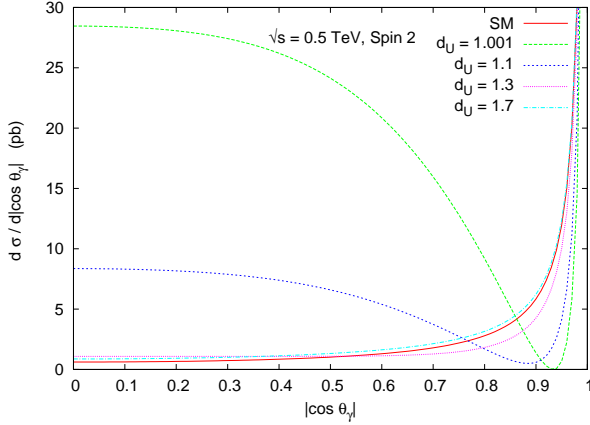


**Fig. 4.** The differential cross section  $\frac{d\sigma}{d|\cos\theta_\gamma|}(e^-e^+ \rightarrow \gamma\gamma)$  versus  $|\cos\theta_\gamma|$  at  $\sqrt{s} = 0.5$  TeV with a spin-2 unparticle exchange plus SM contributions.  $\lambda_2$  is set at 5 for visibility and  $\Lambda_U = 1$  TeV.

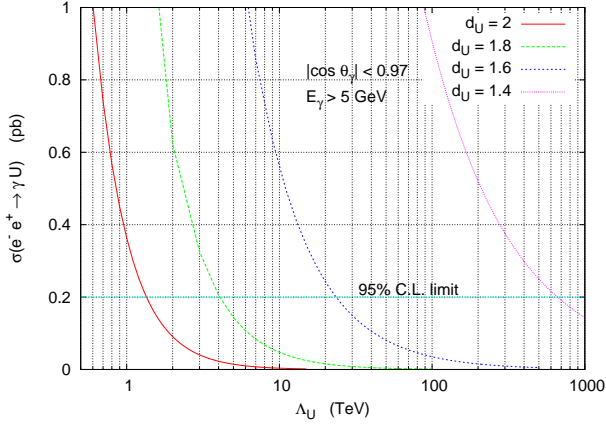


**Fig. 5.** Cross sections for mono-photon plus unparticle production at the  $e^-e^+$  collider with  $\sqrt{s} = 207$  GeV for  $d_U = 1.4, 1.6, 1.8$  and  $2$ . The horizontal line of  $0.2$  pb is the 95% C.L. upper limit.

of the cross section at  $|\cos\theta_\gamma|$  close to 1. When  $d_U$  is less than 1.2 the majority comes from the central region and a dip is formed around  $|\cos\theta_\gamma| \approx 0.9$ . It is because of the spin-2 structure of the operator.

### 3.3 Present constraints

The best limit on single-photon production came from L3 [8], which obtained an 95% C.L. upper limit on  $\sigma(e^-e^+ \rightarrow \gamma + X) \simeq 0.2$  pb under the cuts:  $E_\gamma > 5$  GeV and  $|\cos\theta_\gamma| < 0.97$  at  $\sqrt{s} = 207$  GeV. We calculate mono-photon plus unparticle production with the same cuts in  $e^-e^+$  collisions with  $\sqrt{s} = 207$  GeV versus the unparticle scale  $\Lambda_U$  (with a fixed  $\lambda_1 = 1$ ) for  $d_U = 1.4, 1.6, 1.8$  and  $2$  in Fig. 5. We have also drawn the horizontal line showing the 95% C.L. upper limit (0.2 pb). Since the production cross section scales as  $\lambda_1^2/\Lambda_U^{2d_U-2}$ , the limits increases very rapidly when  $d_U$  decreases from 2 to 1.4 with  $\lambda_1$  fixed.

Since spin-1 unparticle exchanges will lead to 4-fermion contact interactions, we can use the existing

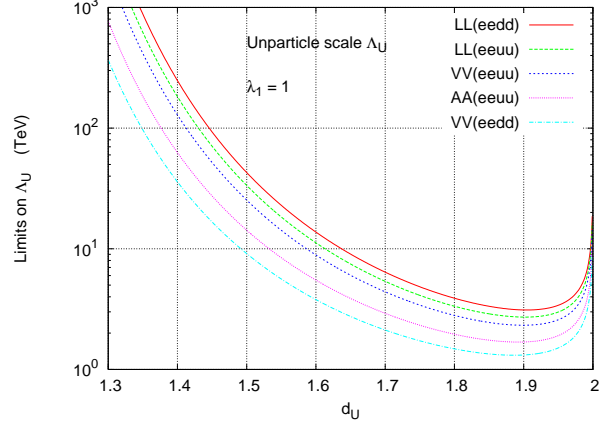


**Fig. 6.** Rescaled limits from existing 4-fermion contact interactions.  $LL$  means only left-left chirality is considered while  $VV$  means  $LL + RR + LR + RL$  and  $AA$  means  $LL + RR - LR - RL$ . We have chosen  $P_U^2 \approx (0.2 \text{ TeV})^2$ .

limits on 4-fermion contact interactions [9, 10] to constrain the unparticle scale  $\Lambda_U$ . We can compare Eq. (11) with the conventional 4-fermion contact interactions

$$\mathcal{L}_{4f} = \frac{4\pi}{\Lambda^2} \sum_{\alpha, \beta=L,R} \eta_{\alpha\beta} (\bar{e}\gamma_\mu P_\alpha e) (\bar{f}\gamma^\mu P_\beta f), \quad (18)$$

which results in the following equality:

$$\lambda_1^2 Z_{d_U} \frac{1}{\Lambda_U^2} \left( -\frac{P_U^2}{\Lambda_U^2} \right)^{d_U-2} = \frac{4\pi}{(\Lambda^{95})^2}, \quad (19)$$

where  $\Lambda^{95}$ s are the 95% C.L. limits on the  $eeqq$  contact interaction scales obtained by combining global data [9]. The best limit is on the  $LL$  chirality because the parity-violating experiments, especially the atomic-parity violation, are very stringent:  $\Lambda_{LL}^{95}(eeuu) \simeq 23$  TeV while  $\Lambda_{LL}^{95}(eedd) \simeq 26$  TeV. The results are shown in Fig. 6.

Phenomenology of unparticle is very rich. While the underlying theory of unparticle is still needed to be unraveled by theorists, experimentalists could detect such a hidden scale invariant sector when the LHC turns on in 2008.

The work was supported in part by the NSC of Taiwan and U.S. DOE.

### References

1. K. Cheung, W.Y. Keung and T.C. Yuan, Phys. Rev. Lett. **99**, (2007) 051803.
2. K. Cheung, W.Y. Keung and T.C. Yuan, Phys. Rev. **D76**, (2007) 055003.
3. H. Georgi, Phys. Rev. Lett. **98**, (2007) 221601.
4. T. Banks and A. Zaks, Nucl. Phys. **B196**, 189 (1982).
5. H. Georgi, Phys. Lett. B **650**, (2007) 275.
6. S. Coleman and E. Weinberg, Phys. Rev. **D7**, 1888 (1973).
7. E. Eichten et al., Phys. Rev. Lett. **50**, 811 (1983); V.D. Barger, et al., Phys. Rev. D **57**, 391 (1998).
8. L3 Coll., Phys. Lett. B **587**, 16 (2004).
9. K. Cheung, Phys. Lett. B **517**, 167 (2001).
10. Particle Data Group, J. Phys. **G33**, 1 (2006).